

# Simulations and tests of superconducting linear bearings for a MagLev prototype

D. H. N. Dias, E. S. Motta, G. G. Sotelo, R. de Andrade, Jr., R. M. Stephan,

L. Kuehn, O. de Haas and L. Schultz

**Abstract**— The complex microstructure of melt grown YBCO bulk material and the non-linear electromagnetic behavior makes it difficult to determine their thermal, electrical and magnetic properties. The knowledge of these parameters is essential to design superconducting magnetic bearings (SMB) for various applications. The main characteristic of a SMB is the levitation force that arises between the superconductor and the magnetic source. The availability of simulation tools can greatly simplify the design of new prototypes. An algorithm based on the critical state model and the Finite Element Method (FEM) was developed. This method is based on the determination of the current density profile within the superconductor due to the penetration of the flux lines. This algorithm showed satisfactory to simulate the levitation force for a rotational magnetic bearing used in a flywheel prototype. In the present paper, this method is used to simulate a linear bearing and to design the optimal geometries for a magnetic rail that is being developed for a MagLev vehicle prototype. The linear bearing consists of two parts: a rail assembled with Nd-Fe-B magnets and YBCO bulks mounted inside a cryostat. Some simulated bearings were mounted and tested. The simulation results agree with the measurements.

**Index Terms**— High-temperature superconductors, Critical state model, MagLev.

## I. INTRODUCTION

Among the applications of high-temperature superconductors (HTS) there are superconducting magnetic levitation systems using the interaction between the magnetic flux lines and the superconducting current within the HTS for stable levitation. The intrinsic property of passive stable levitation makes electronic and power supplies for active controlling superfluous. The Superconducting Magnetic Bearing (SMB) can be designed as a rotating bearing by way of example in flywheel systems, or as a linear bearing for transport systems.

Manuscript received 20 August 2008. This work was supported by CNPq, CAPES, FAPERJ and DAAD.

D. H. N. Dias, R. de Andrade, Jr. and R. M. Stephan are with the Federal University of Rio de Janeiro (e-mail: [ddias@coe.ufrj.br](mailto:ddias@coe.ufrj.br), [randrade@dee.ufrj.br](mailto:randrade@dee.ufrj.br), [richard@dee.ufrj.br](mailto:richard@dee.ufrj.br)).

E. S. Motta is with Federal University of Rio de Janeiro and Indústrias Nucleares do Brasil S. A. – INB (email: [eduardomotta@inb.gov.br](mailto:eduardomotta@inb.gov.br))

G. G. Sotelo is with Federal University of Rio de Janeiro and Faculdade Salesiana Maria Auxiliadora ([sotelo@coe.ufrj.br](mailto:sotelo@coe.ufrj.br))

L. Kuehn, O. de Haas and L. Schultz are with Leibniz Institute for Solid State and Materials Research Dresden (email: [L.Kuehn@ifw-dresden.de](mailto:L.Kuehn@ifw-dresden.de), [O.deHaas@ifw-dresden.de](mailto:O.deHaas@ifw-dresden.de), [L.Schultz@ifw-dresden.de](mailto:L.Schultz@ifw-dresden.de)).

This work will focus on the linear SMB used as the levitation and guidance system of an urban train. This type of chassis has many advantages compared with conventional railway systems and active controlled magnetic bearings. Among the advantages, it can be enumerated: significant reductions of noise, losses, operation and maintenance costs; vehicle without trucks and therefore lighter and; distributed load along the line and not concentrated at the point of contact wheel-rail, implying in reduced infrastructure costs. There are many prototypes of this MagLev vehicle type, showing its feasibility [1,2]. In this context, the Laboratory for Applied Superconductivity (LASUP/UFRJ) is developing an urban vehicle named MagLev-Cobra [1] and the IFW enhanced the fully working prototype named SupraTrans [2].

The main characteristic of a SMB is the levitation force between the superconductor and the magnetic field source. An algorithm based on the critical state model and Finite Element Method (FEM) was implemented [3]. This methodology determines the current density profile within a superconductor due to the penetration of magnetic flux lines. The simulated results match very well with the measured values for two axially symmetric SMB's [4, 5].

The technique of combining a FEM module with an algorithmic language was used to simulate linear SMB's. The simulation is performed to MagLev levitation system vehicle prototypes, considering two types of Nd-Fe-B permanent magnets (PM) rails and one three seeded cuboidal YBCO bulk. The linear SMB where mounted and measured to verify the applicability of the developed methodology to calculate the levitation force.

## II. LINEAR BEARING MODELING

In this section the method used to simulate a superconducting linear bearing is presented. This method consists in modeling the superconductor material and the magnetic rail. Two different arrangements of the PM were analyzed and are shown in Fig. 1. The coordinate system used to describe motion sequences for transport system is also shown in this figure, where the  $x$  is pointed in the main direction of motion, lateral displacements are in  $y$  direction and  $z$  indicates displacements in vertical direction.

The rail showed in Fig. 1(a) is composed by Nd-Fe-B permanent magnets of 1"x1"x0.5" with magnetization in  $z$  direction. The coercive force ( $F_c$ ) of these PM's is 891kA/m. With respect of the direction of magnetization, this rail is

called *Up-Down* (UD). Between the PM's an aluminium bar (spacer) is placed and below them an iron back yoke improves the magnetic flux density in the top of the system and helps the assemblage process.

The rail showed in Fig. 1(b) is composed by equal permanent magnets, with magnetization in the  $y$  direction. This rail consists of three soft magnetic (SM) elements (Iron) to collect the magnetic flux and two PM's. The concentration of the flux density above the soft magnetic elements increases the flux gradient and the absolute value of the flux on the surface. In terms of flux concentration, this rail is called *Flux Collector or Flux Shaper* (FS).

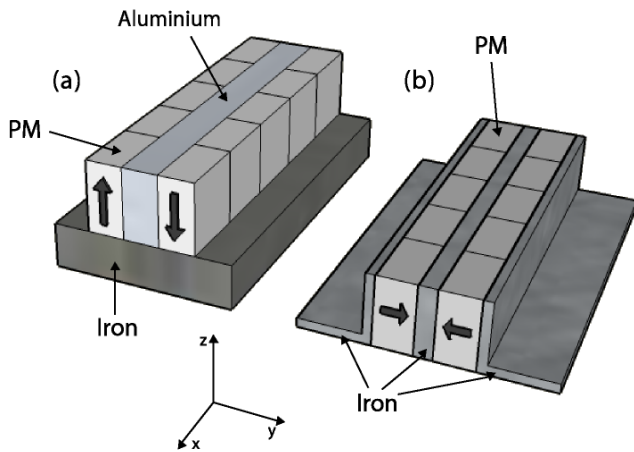


Fig. 1. Geometry of the permanent magnetic rails: (a) UD rail and (b) FS rail.

The simulations were performed with commercial FEM software using 2D magnetostatic solutions. Both geometries (UD and FS) were simulated taking into account the lateral section symmetry along the main moving direction ( $x$  direction). The position of the HTS bulk above the magnetic rail is shown in Fig. 2. The width of both rails is 38.1 mm and the dimensions of the used Nd-Fe-B magnets are equal in volume. The different magnetic field distributions are shown in Fig. 2 for the system (a) with UD magnetization and the system (b) for the rail with FS.

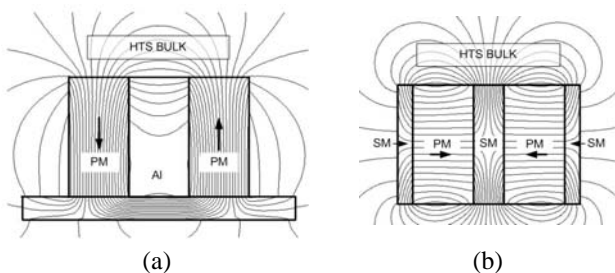


Fig. 2. Position of the HTS bulk within the magnetic field above the (a) UD rail and (b) FS rail

The simulated and measured results for the  $z$  component of the magnetic flux density  $\mathbf{B}$  can be seen in Fig. 3(a) for UD rail and Fig. 3(b) for FS. The absolute value of the  $z$  component of  $\mathbf{B}$  above the pole is roughly two times higher in the case of the FS rail compared with the UD rail.

Due to the higher absolute value of  $\mathbf{B}$  and the large gradient  $\text{dB}/\text{dz}$ , a higher levitation force for the FS rail can be expected.

During the mounting of the FS rail, a mechanical process caused the heating of the PM's and a consequent reduction in its magnetization. Due to this reason, the coercive force of the PM was reduced to 626kA/m. Since the model is able to give the correct distribution of flux line and the magnitude of  $\mathbf{B}_z$  is in accordance with the measurements, the next step is to find a way to simulate the superconductor material.

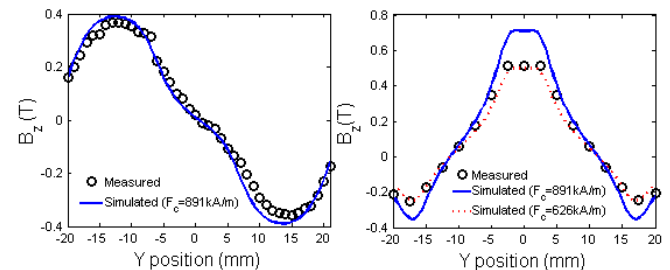


Fig. 3. Magnitude of the  $z$  component of the magnetic flux density  $\mathbf{B}$  for: (a) UD and (b) FS rail. The solid lines are the simulated results and the circles ones are the measured results. In both case the gap was 2 mm.

For a type II superconductor, when the applied field has a value between  $H_{c1}$  and  $H_{c2}$ , the material is not a perfect diamagnetic. The flux lines can partially penetrate the material without destroying the superconductivity through the vortices. These vortices are surrounded by a microscopic current density. Due to the complexity of the problem, models that consider the vortex become prohibitive for a practical purpose. As FEM software cannot be used directly to simulate the HTS, the following procedure was developed to calculate a current density distribution inside a superconductor using any commercial FEM package. To represent the superconductor material, a method based on the critical state model [3], known as Bean model [6] was used. The Bean model [6] considers that the microscopic current density of the vortices can be substituted by a constant macroscopic current density  $J_c$ . Therefore the electromagnetic behaviour inside the superconductor can be represented by a non-linear behaviour  $\mathbf{E}-\mathbf{J}$ , as presented by equations (1) and (2).

$$\mathbf{J} = J_c \frac{\mathbf{E}}{|\mathbf{E}|} \quad \text{if } |\mathbf{E}| \neq 0, \quad (1)$$

$$\frac{\partial \mathbf{J}}{\partial t} = 0 \quad \text{if } |\mathbf{E}| = 0. \quad (2)$$

In order to implement this model a complementary formalism through the magnetic potential  $\mathbf{A}$  is introduced [7]. The expression for the electrical field can be evaluated by using Faraday's Law together with the definition of  $\mathbf{A}$  ( $\mathbf{B} = \nabla \times \mathbf{A}$ ). The magnetic vector potential may be divided in two components and the expression for the electrical field can be written as:

$$\mathbf{E} = -\frac{\partial \mathbf{A}_{ext}}{\partial t} - \frac{\partial \mathbf{A}_{sc}}{\partial t}, \quad (3)$$

where  $\mathbf{A}_{ext}$  is due to the permanent magnets and  $\mathbf{A}_{sc}$  is due to the current density in the superconductor  $J_{sc}$ . The relation between  $\mathbf{A}_{sc}$  and  $J_{sc}$  can be established by the Poisson equation:

$$\nabla^2 \mathbf{A}_{sc} = -\mu_0 \mathbf{J}_{sc}. \quad (4)$$

The superconductor region is divided in a mesh with  $N$  elements and equation (4) was solved considering an unitary current density in each element. After that, the superposition principle is applied to substitute the Poisson equation by the following relation [8]:

$$[A_{sc}] = [M][J_{sc}]. \quad (5)$$

The matrix  $[M]$  and the vector  $[A_{ext}]$  are obtained using FEM. Matrix  $[M]$  has dimension  $N \times N$ . Each column of  $[M]$  contains the information of  $[A_{sc}]$  for all elements in the superconductor mesh due to the unitary current density applied in a single element. The vector  $[A_{ext}]$  has the information of the field generated by the linear bearing.

The method consists in solving (3) and (5) together with the non-linear relation  $\mathbf{E}-\mathbf{J}$  from numerical results obtained through FEM software. Equation (3) can be rewritten applying an approximation for the derivate as:

$$[E_{AV}^t] = -\frac{[M](J_{sc}^t - J_{sc}^{t-1})}{\Delta t} - \frac{[A_{ext}^t] - [A_{ext}^{t-1}]}{\Delta t}. \quad (6)$$

Equation (6) will be solved to determine the current density in each element of the superconductor mesh and then the magnetic levitation force is calculated using the information of  $\mathbf{B}_{tot}$ , due to the superconductor and the linear bearing, through the integral equation given by the Lorentz force:

$$F_z = \int \mathbf{J}_x \times \mathbf{B}_{y_{tot}} dV. \quad (7)$$

Fig. 4 shows a block diagram that resume the numerical implementation to calculate the current density profile in the superconductor. This procedure can be well understood in [5].

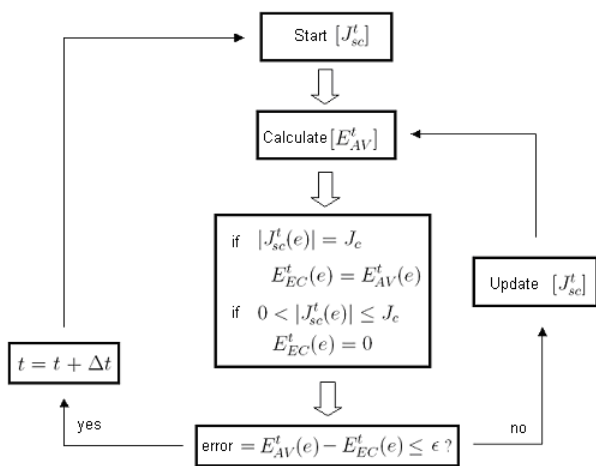


Fig. 4. Block diagram resuming the process to calculate the current density profile in the superconductor.

### III. RESULTS

One YBCO bulk was used for testing with both rails and comparison with the simulated results. A multi-seeded (3 seeds) YBCO bulk with the green body size of  $40 \times 100 \times 20$  mm<sup>3</sup> and a final size of  $31 \times 83 \times 5$  mm<sup>3</sup> was used. The sample was doped with Pt to improve the pinning force. The quality of the sample was evaluated by scanning the trapped field after magnetization with a Nd-Fe-B magnet with a magnetic field of 0.4 T on its surface. The field cooling process at 77 K

has been used. The results of the scan in a distance of 0.5 mm above the surface are shown in Fig. 5. The three pyramidal surfaces are typical for a three-seeded, textured YBCO bulk. The high gradient of the trapped magnetic field profile indicates a high critical current density  $J_c$ . With the relation

$$F_z \propto J_c, \quad (8)$$

a high levitation pressure ( $> 5 \text{ N/cm}^2$ ) can be expected.

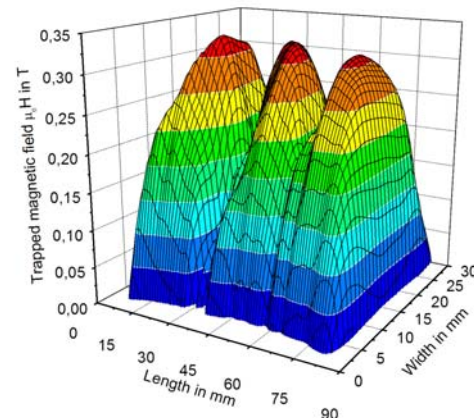


Fig. 5. Magnetic scan of the trapped field in the YBCO bulk at 77K.

An experimental rig was used to compare the simulation results with measurements, as shown in Fig. 6. An automatic data acquisition system, that uses a load cell for the force measurement, makes the operation easy. The YBCO bulk was fixed on the bottom of the cryostat by mechanical clamp. The tests were done starting the cryostat in an initial position of 50mm from the magnetic rail, where the influence of its magnetic field can be neglected. The YBCO block inside the cryostat was cooled with LN<sub>2</sub> without the presence of the rail magnetic field (ZFC– Zero Field Cooling). After that, the cryostat was approximated very slowly ( $v \sim 1 \text{ mm/s}$ ) to the linear bearing, in a quasi-static process, until a minimum gap of 4 mm was reached. Finally, the cryostat was elevated and returned to the initial position.



Fig. 6. Experimental rig used during the measurements.

Fig. 7 shows the measured and simulated results for the magnetic levitation force of the UD rail. The model predicts accurately the levitation force and the hysteretic behavior.

Fig. 8 shows the results obtained for the FS rail, for two values of coercive force. For the same PM used in the UD rail, the behavior of the levitation force is not precisely predicted. With the coercive force of the PM's adjusted to 626kA/m, due to the reduced magnetization after the mounting process of the rail, the maximum value of the levitation force and the hysteretic behavior prediction could be improved.

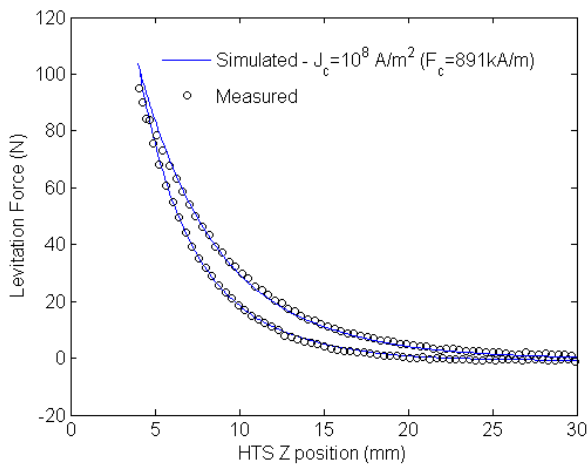


Fig. 7. Magnetic levitation force measurements (circles) compared with the simulated results (solid line) for the UD rail.

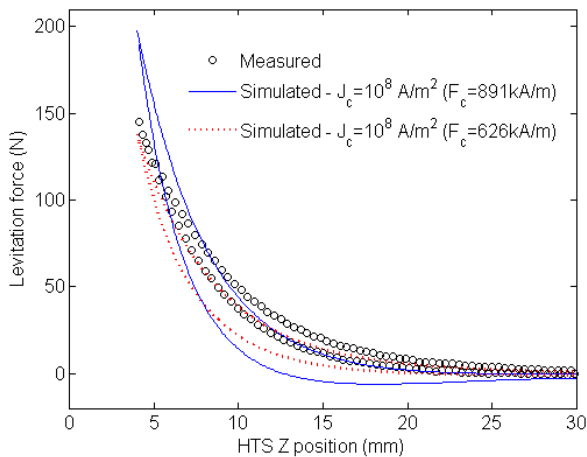


Fig. 8. Magnetic levitation force measurements (circles) compared with the simulated results for  $F_c=891\text{kA/m}$  (solid line) and for  $F_c=626\text{kA/m}$  (dashed line) for the FS rail.

#### IV. CONCLUSIONS

This work has compared simulations and measurement results for linear superconducting magnetic bearings. The algorithm used in the simulation model is based on the critical state model. It evaluates the current profile within a superconductor bulk due to external magnetic field and calculates the levitation force.

The simulations and measurements were performed for two types of magnetic rails. The simulation of the Up-Down rail configuration was able to predict the levitation force and also its hysteretic behavior, with maximum relative discrepancy of 8% at 4mm gap. For the Flux Shaper rail, after the coercive force correction, levitation force and its hysteretic behavior fitted with the measurements with a maximum relative discrepancy of 26% in the approaching curve.

This model showed its applicability to develop real size SMB for MagLev systems. The next step is to apply the algorithm, presented here, to simulate further non-usual configurations.

#### REFERENCES

- [1] E. G. David, R. M. Stephan, G. C Costa, A. C. Ferreira, R. de Andrade Jr., Nicolsky, and M. A. Cruz Moreira, "A Feasibility study of an HTS-Maglev line at the Federal University of Rio de Janeiro", Proceedings of MAGLEV'2006 – The 19<sup>th</sup> International Conference on Magnetically Levitated Systems and Linear Drives, 13-15 September, 2006, Dresden, Germany.
- [2] L. Schultz, O. de Haas, P. Verges, C. Beyer, S. Röhlig, H. Olsen, L. Kühn, D. Berger, U. Noteboom, U. Funk, " Superconductively levitated transport system - the SupraTrans project", IEEE Trans. Appl. Supercond., vol. 15, pp. 2301-2305, Jun. 2005.
- [3] D. Ruiz-Alonso, T. A. Coombs and A. M. Campbell, "Numerical Analysis of High-Temperature Superconductors with the critical-state model", IEEE Trans. Appl. Superconduct., vol. 14, n. 4, December 2004.
- [4] G. G. Sotelo, R. de Andrade, Jr., and A. C. Ferreira, "Test and simulation of superconducting magnetic bearings", submitted to IEEE Transactions on Applied Superconductivity in 2008.
- [5] G. G. Sotelo, "Modelagem de Supercondutores aplicada ao projeto de mancais magnéticos", PhD thesis, COPPE, Federal University of Rio de Janeiro, Rio de Janeiro, May 2007 (in portuguese).
- [6] C. P. Bean, "Magnetization of high-field superconductors", Review of Modern Physics, vol. 36, pp. 31-39, January 1964.
- [7] S. J. Salon, Finite element analysis of electrical machines, Rensselaer Polytechnic Institute, Troy, New York.
- [8] G. Barnes, M. McCulloch, and D. Des-Hughes, "Computer modelling of type II superconductors in applications", Superconductor Science and Technology, vol. 12, pp. 518-522, 1999.